

Landslides (2020) 17:301–312
 DOI 10.1007/s10346-019-01283-8
 Received: 15 January 2019
 Accepted: 13 September 2019
 Published online: 24 October 2019
 © Springer-Verlag GmbH Germany
 part of Springer Nature 2019

Jiren Xie · Taro Uchimura · Gonghui Wang · Quan Shen · Zain Maqsood · Canrong Xie ·
 Jiapeng Liu · Weikai Lei · Shangning Tao · Pan Chen · Hongyuan Dong · Guoxiong Mei ·
 Shifan Qiao

A new prediction method for the occurrence of landslides based on the time history of tilting of the slope surface

Abstract In recent decades, early warning systems using tilt sensors to predict the occurrence of landslides have been developed and employed in slope monitoring due to the simple installation and low cost of these systems. However, few studies were carried out to investigate the tilting behaviors of landslides, and the prediction methods for the occurrence of slope failure based on tilting measurements also demand detailed investigations. In this paper, pre-failure tilting behaviors of slopes were investigated by performing a series of model tests as well as a field test. The test results reveal a linear relationship between the reciprocal tilting rate and time during the acceleration stage of tilting before slope failure. Furthermore, an equation for this linear relation was also proposed. By approximating the reciprocal tilting rate to be αt^α , the slope failure time can be forecasted using the proposed equation, and the predicted failure time is consistent with the actual slope failure time recorded in this study. Additionally, the correlation between the tilting rate and remaining time before slope failure in logarithmic space was also studied, and most of the data is situated in a region with boundaries. Based on this region, it is possible to anticipate the remaining time before slope failure at an arbitrary tilting rate in the acceleration stage. Conclusively, this paper provides comprehensive investigations on the correlation between the pre-failure tilting behaviors and duration time before landslides, and also introduces a method to potentially predict the occurrence of slope failure based on the slope tilting measurement.

Keywords Tilting behaviors · Slope failure · Accelerating stage of tilting · Tilting rate · Duration time

Introduction

Non-seismically triggered landslides have induced serious losses of properties and human lives, for example at least 4718 recorded deaths and nearly \$980 million were caused by landslides during the period from 2004 to 2016 (Petley 2012; Zhang and Huang 2018). To reduce the number of fatalities and economic losses associated with landslides, low-cost early warning systems for slope failure have been developed in recent decades, and considered as promising approaches to mitigate the losses induced by landslides (Intrieri et al. 2012; Uchimura et al. 2015; Dixon et al. 2018).

The landslide prediction is a complex task, and longstanding effort has been made to increase the confidence of predictions (Saito 1969; Fukuzono 1985; Federico et al. 2015; Manconi and Giordan 2016; Intrieri and Gigli 2016; Intrieri et al. 2019). Some real-time early warning systems were proposed to issue the warning for landslides during the storm by utilizing the correlation between the rainfall intensity and risks of landslides (Keefer et al.

1987; Okada 2001; Kuramoto et al. 2005; Osanai et al. 2010). These real-time early warning systems work well to evaluate the likelihood of potential landslides in a region, but they are not effective to predict the slope failure of an individual slope within the region. Additionally, some other early warning systems were also developed using Soil Moisture Index (SMI), which has been adopted as an indication for early warning by Japanese local governments since 2008 (Ishihara and Kobatake 1979; Okada 2001; Osanai et al. 2010). However, these systems are not applicable to anticipate the occurrence of landslides due to the abstruse relationship between the soil moisture content and stability of slopes.

The typical early warning systems of landslides are based on the displacement measurement at slope surfaces (Angeli et al. 2000; Petley et al. 2005; Intrieri et al. 2012). Some landslide forecasting methods for these monitoring systems were also developed, which were deduced from the relationship between the displacement rate or reciprocal displacement rate and duration time in the accelerating stage before the slope failure (Saito 1969, 1987; Fukuzono 1985; Voight 1988, 1989; Petley et al. 2002; Okamoto et al. 2004; Mufundirwa et al. 2010; Hao et al. 2016; Carlà et al. 2017). The general expression for these methods can be given as (Fukuzono 1985)

$$\frac{1}{v} = [a \cdot (a-1)]^{\frac{1}{\alpha-1}} (t_f - t)^{\frac{1}{\alpha-1}} \quad (1)$$

Where $\frac{1}{v}$ means the reciprocal displacement rate, a and α are constant parameters. It was reported that the value of α in Eq. 1 is close to 2 (Saito 1969; Voight 1989). t in this equation represents time, while t_f is the slope failure time at which the displacement rate becomes infinite.

The landslide forecasting methods using Eq. 1 based on surface displacement measurements have been validated by laboratory tests and some field events (Fukuzono 1985; Petley et al. 2002; Mufundirwa et al. 2010; Carlà et al. 2017; Intrieri et al. 2019). However, limitations associated with these techniques are also existing, such as the complexity in installation and maintenance of these monitoring systems (Uchimura et al. 2015; Smethurst et al. 2017).

Some researchers also developed the slope early warning systems with the measurement of acoustic emission generated by deforming soil (Koerner et al. 1981; Rouse et al. 1991; Smith et al. 2014; Dixon et al. 2018). Waveguides are typically employed in these systems to mitigate the attenuation of acoustic emissions in propagation, and granular backfill materials are placed around the waveguides to generate the acoustic emissions when slopes deform. However, the effectiveness of these systems in landslide prediction is still under investigation.

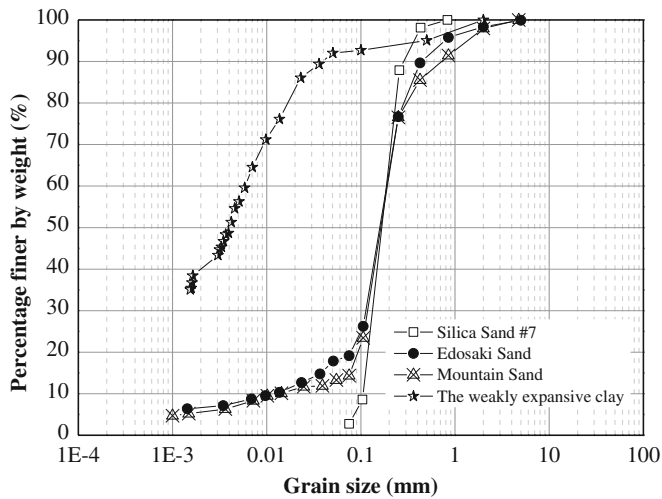


Fig. 1 Particle size distribution of Materials

In recent years, with the development of microelectronic techniques, new early warning systems using MEMS (Micro Electro Mechanical Systems) technology were proposed to estimate the risk of slope failure by observing the tilting behaviors at the slope surface in unstable parts of slopes (Towhata et al. 2005; Uchimura et al. 2010; Dikshit et al. 2018). Although the tilting measurement systems have been used in some field events because of the simple installation and low cost (Voight 1988; García et al. 2010; Uchimura et al. 2015; Xie et al. 2019), detailed investigations on the landslide

prediction methods based on tilting measurements at slope surfaces were rarely performed.

In this paper, comprehensive investigations on the tilting behaviors of landslides, and the method to predict the occurrence of slope failure using tilting measurements at slope surfaces, were carried out by performing a series of laboratory model tests as well as a field test. Two typical small scale laboratory tests were conducted under different testing conditions, and the slope failure in these two model tests was induced by applying constant artificial rainfall. In Model Test 1, tilt sensors were installed in the slope with a pre-defined circular slip surface to detect the tilting behaviors at the slope surface in rotational landslides. The slope model in Model Test 2 was comprised of two layers with different dry density, and tilt sensors together with long rods were employed in this test to measure the tilting behaviors in shallow landslides with a planar slip surface. In addition, a big scale model test was also carried out, in which the slope failure was triggered by water infiltration from the back of the slope. The tilting behaviors of the slope were measured by tilt sensors with the length of 20 cm installed in the slope. Furthermore, a field test was performed on a natural slope, and the slope failure in this field test was also triggered by applying constant rainfall. The tilting behaviors of the unstable part in this field test were recorded by the tilt sensor attached to a short rod with a length of 7 cm. In all of these tests, the tilting behaviors of slopes along the slope direction were monitored by the tilt sensors which were connected to a data logger for continuous data recording. The frequency for data sampling in Model Test 1, Model Test 2 and the field test was 1 Hz, while that in Model Test 3 was 1/60 Hz.

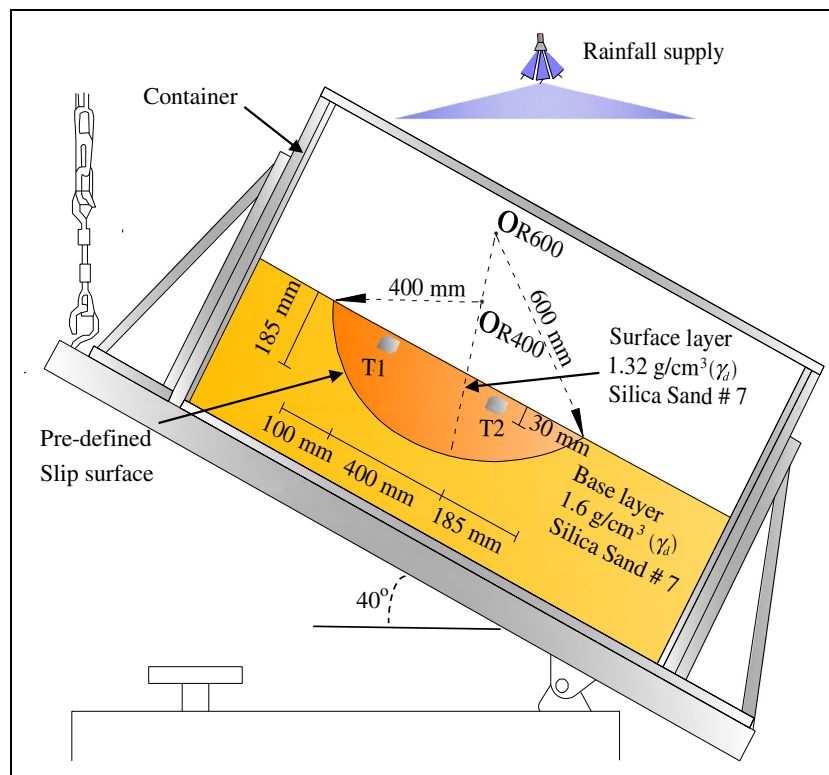


Fig. 2 The cross section of the slope model and the arrangement of apparatuses in Model Test 1

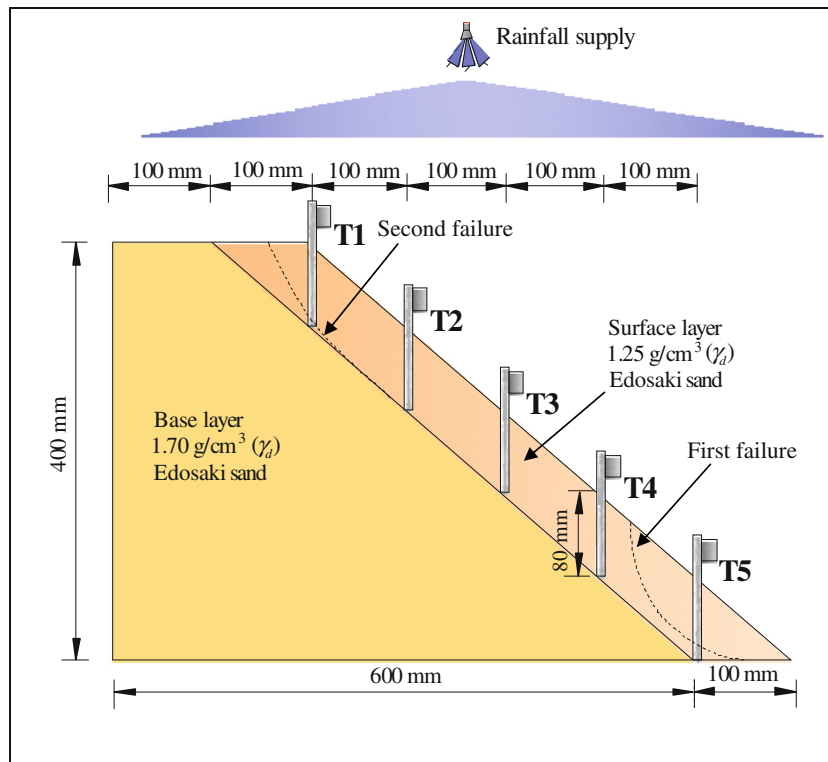


Fig. 3 The cross section of the slope model and the setup of apparatuses in Model Test 2

Methodology and materials

To examine the tilting behaviors of different types of landslides, three typical types of laboratory model tests and a field test were carried out.

Laboratory model tests

Model test 1

In this model test, the slope model was built in a rectangular box, sized 1165 mm in length, 450 mm in width, and 380 mm in height. This slope model was comprised of a base layer and a surface layer, which was made of Silica sand # 7 (Fig. 1) with different dry density (1.60 g/cm^3 for the base layer and 1.32 g/cm^3 for the surface layer). The G_s of Silica sand #7 was 2.63 determined by the Density Bottle Method according to Japanese Standards. The permeability of the surface layer was $1.06 \times 10^{-2} \text{ cm/s}$ and it was $4.5 \times 10^{-3} \text{ cm/s}$ in the base layer. The schematic illustration for the cross section of the slope model and the arrangement of apparatuses employed in this test are presented in Fig. 2. When making the base layer, the sand with a water content of 10% was compacted to the designed dry density of 1.60 g/cm^3 which approximates to the maximum dry density. Afterwards, the base layer was carved into a pre-defined shape to construct the sliding surface. The pre-defined shape was curvilinear and consisted of two circular parts with different radii, 400 mm in the upper part and 600 mm in the lower part respectively (Fig. 2). Subsequently, the surface layer was built on the base layer with a polythene sheet placed between them performing as the pre-defined slip surface of the slope model due to the fact that the polythene sheet can reduce friction and restrict water flow. After building the slope model, two tilt sensors (T1 and T2) as shown in Fig. 2, were buried in the slope with the depth of 3 cm to measure the tilting

behaviors of the slope. Details for T1 and T2 are provided in Fig. 2. In next step, the slope model was tilted to an angle of 40° using the lifting chain fixed at one end of the container, and then artificial rainfall was applied with a constant rainfall intensity of 70 mm/h to induce the slope failure.

Model test 2

The illustration of this test and the arrangement of the instruments are presented in Fig. 3. As shown in Fig. 3, the slope model consisted of the base layer and surface layer, which were made of Edosaki Sand procured from a natural slope in Ibaraki Prefecture of Japan (Fig. 1). The G_s of this sand was 2.68, and the permeability for the surface layer was $4.70 \times 10^{-3} \text{ cm/s}$ while that for the base layer was less than $1 \times 10^{-3} \text{ cm/s}$. The base layer of the slope model was made of Edosaki sand with a water content of 14.6%, and the dry density in this layer was about 1.70 g/cm^3 close to the maximum dry density of this material. Compared with the base layer, the surface layer was built with looser dry density around 1.25 g/cm^3 , and the initial water content in this layer was 10%. The thickness of the surface layer was 100 mm with the inclination of 36° . Five tilt sensors were inserted into the surface layer, and the interval between these tilt sensors was 100 mm at horizontal direction as shown in Fig. 3. In this test, the slope failure was also induced by applying artificial rainfall with the constant rainfall intensity of 70 mm/h .

Model test 3

A big scale model test was conducted at Public Works Research Institute (PWRI), Tsukuba, Japan. The model slope was made of the mountain sand with a dry density of 1.39 g/cm^3 , and the permeability of the slope

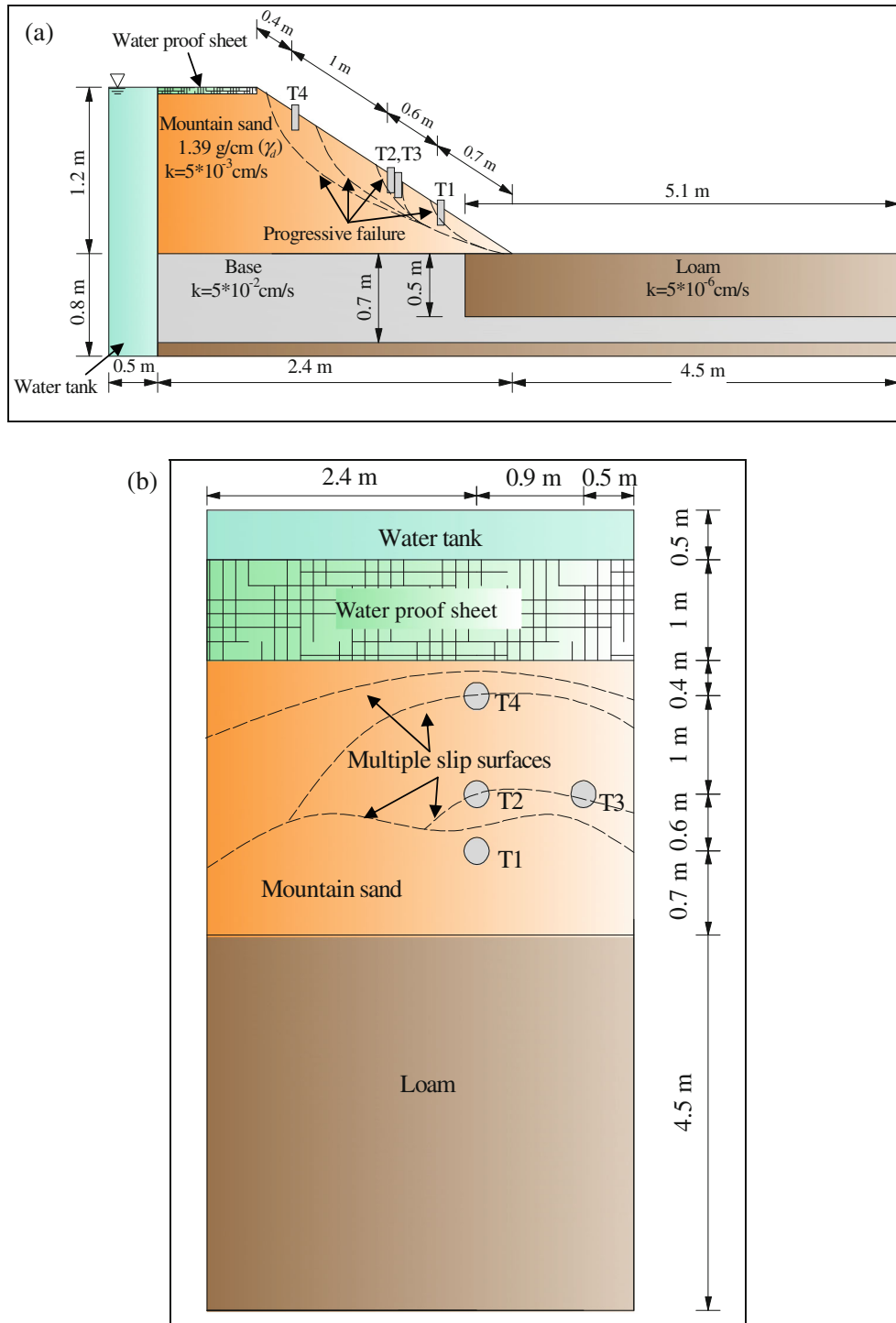


Fig. 4 Model Test 3: (a) The cross section of the slope and arrangement of sensors, (b) The front view of the slope and arrangement of sensors

was 5×10^{-2} cm/s. The particle size distribution of the mountain sand is presented in Fig. 1. The slope model had a gradient of 2:1, and the size was 2.4 m in length, 3.8 m in width and 1.2 m in height as shown in Fig. 4. The main part of the slope model was built on a base, of which the permeability was 5×10^{-3} cm/s, while the toe of the slope model was located on a layer made of loam with the permeability of 5×10^{-6} cm/s. There was a water tank filled with

water set at the back of the slope model to reproduce the situation of a river with a constant water level. On the crest of the slope, water proof sheets were placed. Four tilt sensors were installed in this slope model with the length of 0.2 m, and the exact locations of these sensors are indicated in Fig. 4a and Fig. 4b. In this model test, the slope failure was caused by the water infiltration from the back of the slope.



Fig. 5 The image of the testing slope in the field test

A field test

A field test was also performed on a natural slope in Baise city of Guangxi province, China (Fig. 5). The natural slope was comprised of weakly expansive clay and the particle size distribution of the material is provided in Fig. 1. The slope angle was around 40°, and the high slope stability at such a steep angle was attributed to the strong structure of the expansive clay. A trench was excavated at the toe of the slope with a depth of 0.2 m to make the slope easier to collapse. Six tilt sensors with different lengths were installed in the slope as shown in Fig. 6. After the installation of tilt sensors, artificial rainfall was applied with a constant rainfall intensity of 21 mm/h, and the major failure occurred in the middle part of the slope four hours later.

Test results

Results of model test 1

In this test, the slope failure was triggered by applying artificial rainfall, and the slope slid along the pre-defined slip surface. The tilt sensors, T1 and T2, which were installed in the surface layer above the slip surface, tilted backward when the slope was sliding. In this study, if the tilt sensors tilt backward, positive tilting angles could be observed. Images of the slope before and after the slope failure are presented in Fig. 7. Figure 8 shows the time history of tilting measured by T1 and T2. As shown in Fig. 8, prior to the slope failure, an accelerating stage of tilting is indicated with the duration time of 7 min. In addition, the relationship between the reciprocal tilting rate and the time is presented in Fig. 9. The method for the calculation of the reciprocal tilting rate is provided in Appendix of this paper. Figure 9 reveals linear relationships between the inverse number of the tilting rate and time, and the fitting lines for the linear relationships are also indicated in this figure. Accordingly, the slope failure time can be predicted using the fitting line of T1 and T2 when the reciprocal tilting rate becomes 0 min/°. The predicted slope failure time calculated by utilizing the fitting line of T1 and T2, is 47.37 min and 47.47 min respectively, which is noticeably comparable to the actual failure time of the slope in this test, 47.28 min as shown in Fig. 9.

Results of model test 2

The slope failure of Model Test 2 was also induced by applying artificial rainfall with the rainfall intensity of 70 mm/h. Figure 10 shows the images of the slope model before and after the landslide. The failure

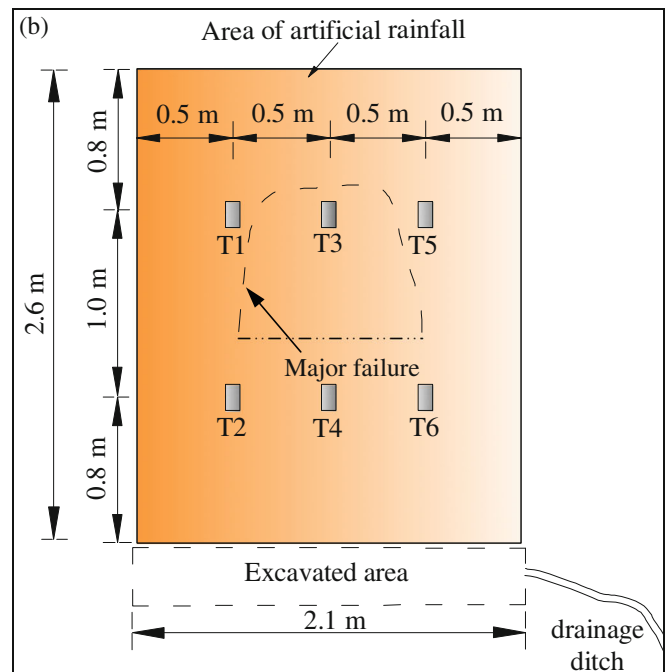
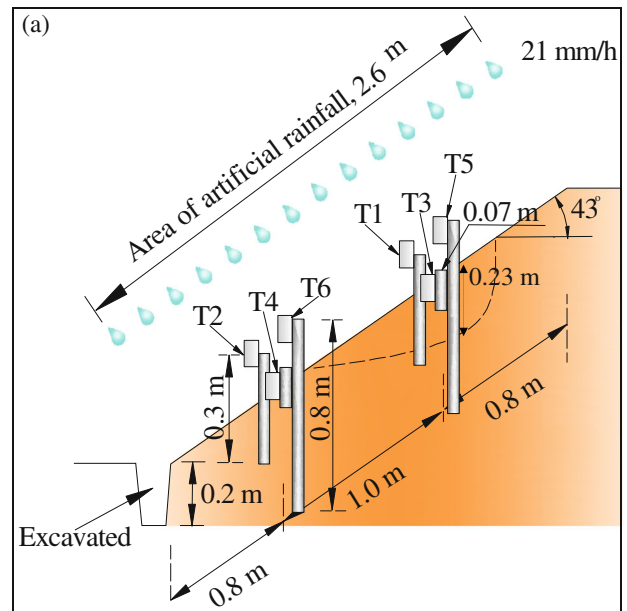


Fig. 6 The field test: (a) The cross section of the slope and setup of tilt sensors, (b) The front view of the slope and setup of tilt sensors

process of the slope in this test is indicated in Fig. 3. As shown in Fig. 3, the slope failure began at the bottom part of the slope before the second failure occurred, and the tilting behaviors of the slope in the first failure was recorded by tilt sensor T5 together with a rod reaching to the depth of the slip surface. After the first failure, the remaining part collapsed subsequently. The tilting behaviors of the slope in this progressive slope failure measured by tilt sensors are presented in Fig. 11. As shown in Fig. 11(b), an accelerating stage of tilting was first detected by T5, and then measured by T4 and T3. The tilting behaviors of the slope measured by T1 and T2 located in the upper part of the slope, were influenced by the deposition of the failed soil at the lower part as shown

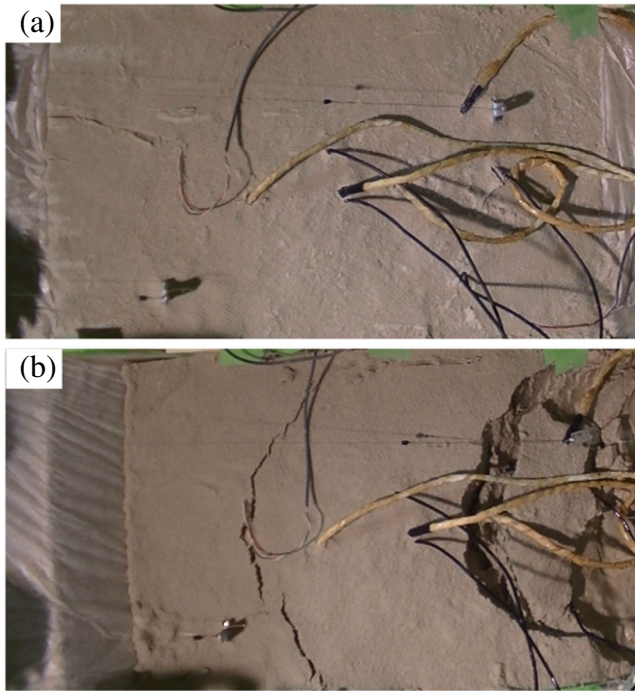


Fig. 7 Images of Model Test 1: (a) The image of the slope before failure, (b) The image of the slope after failure

in Fig. 10(b). Correlations between the inverse number of the tilting rate and time in the acceleration stage of tilting measured by T5, T4 and T3 are indicated in Fig. 12. Linear relations between the reciprocal tilting rate and time are revealed, and the fitting lines for these line relations are also presented in this figure. The slope failure time was computed by using the fitting line of T5, T4 and T3 when the reciprocal tilting rate becomes 0 min/deg, which is 46.33 min, 47.17 min and 46.57 min respectively. Although the slope failure time forecasted based on the data of T3 and T4 is also close to the actual failure time of the first slope failure (46.58 min), the authors suggest to predict the occurrence of landslips in the progressive failure process, using the monitoring data from first

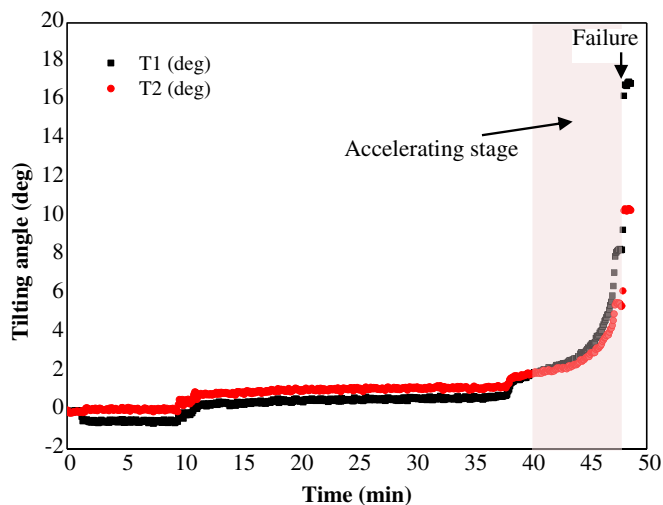


Fig. 8 Time history of tilting of the slope surface measured by tilt sensor, T1 and T2

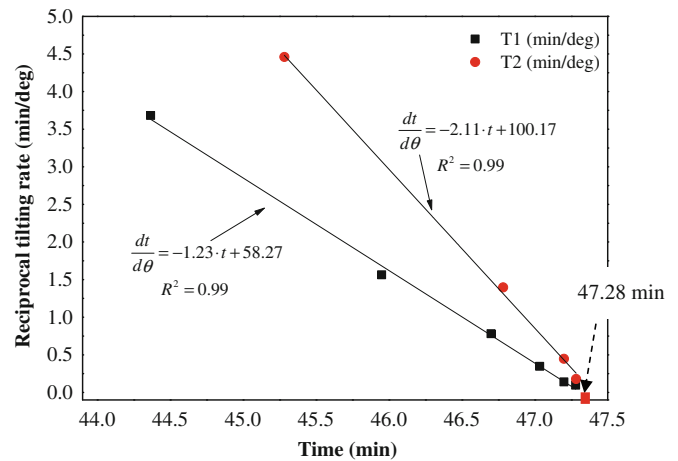


Fig. 9 The reciprocal tilting rate against time of the accelerating stage

slope failure (the data of T5 in this study) on the conservative side. Furthermore, the tilting behavior measured by T5 is more reliable than that measured by T4 and T3, which might be influenced by the deposition of the failed part from the first slope failure.

Results of model test 3

Progressive slope failure also occurred in this test with multiple slip surfaces, which was triggered by water infiltration from the back of the slope as shown in Fig. 4. Figure 13 indicates the images of the slope model before and after the failure, while the time history of tilting of the slope surface measured by tilt sensors is presented in Fig. 14. The slope failure began at the toe of the slope where tilt sensor

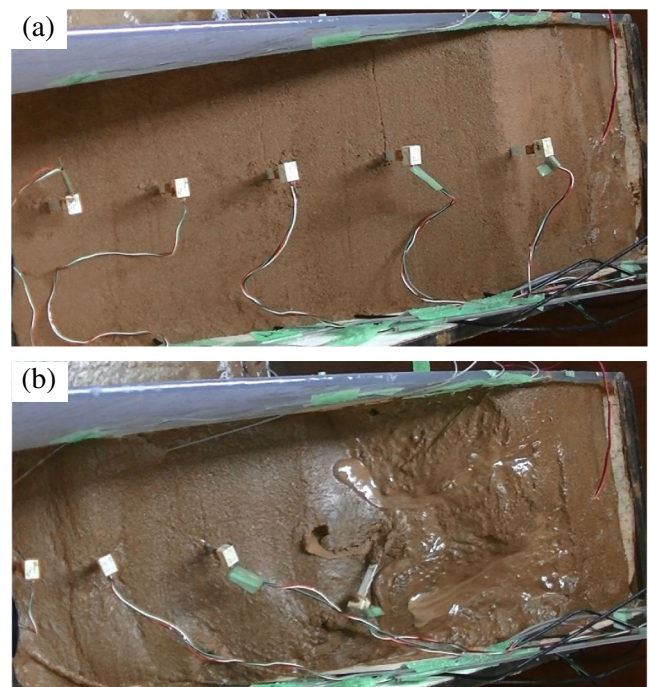


Fig. 10 Images of Model Test 2: (a) The image of the slope before failure, (b) The image of the slope after failure

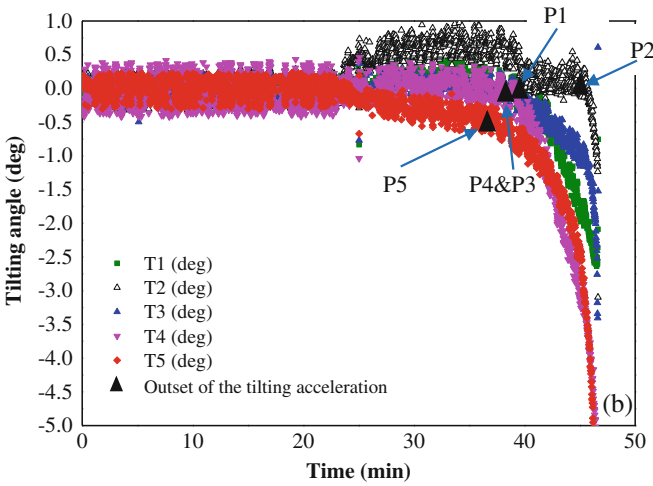
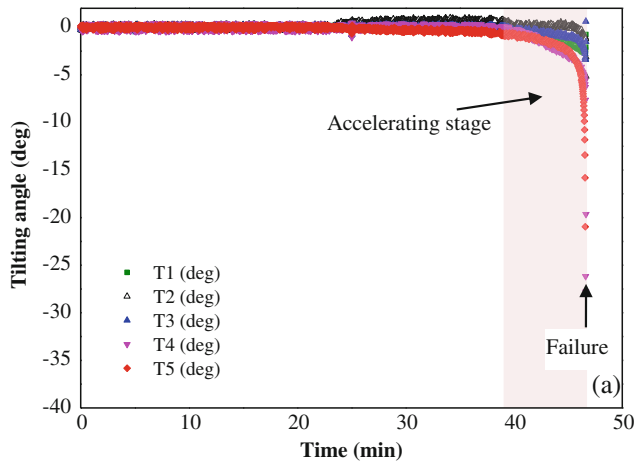


Fig. 11 Time series of the tilting angle: (a) Time history of the slope tilting measured by tilt sensors, (b) Enlargement of Fig. 11(a) with smaller ranges of tilting angles

Fig. 13 Images of big scale model test: (a) The image of the slope before failure, (b) The image of the slope after failure

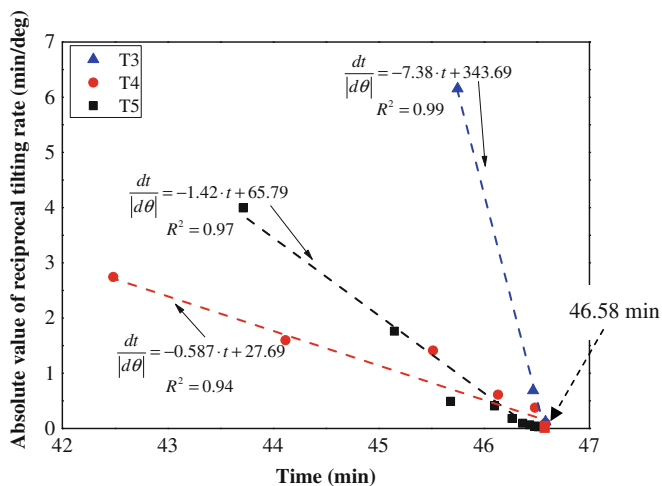


Fig. 12 The reciprocal tilting rate against time prior to the slope failure

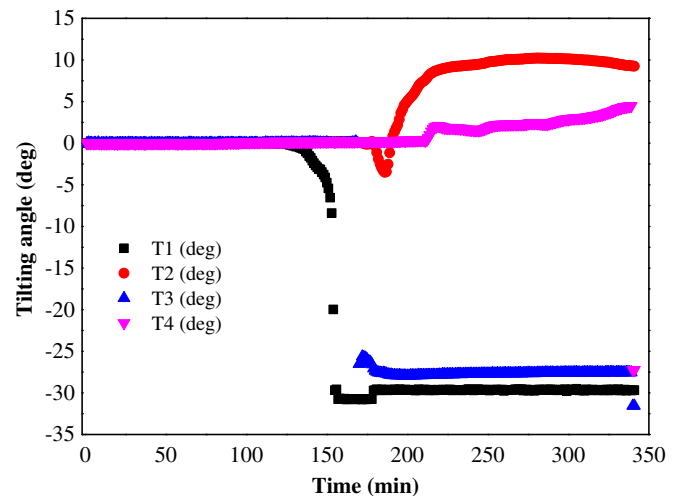


Fig. 14 Time history of tilting of the slope surface measured by four tilt sensors

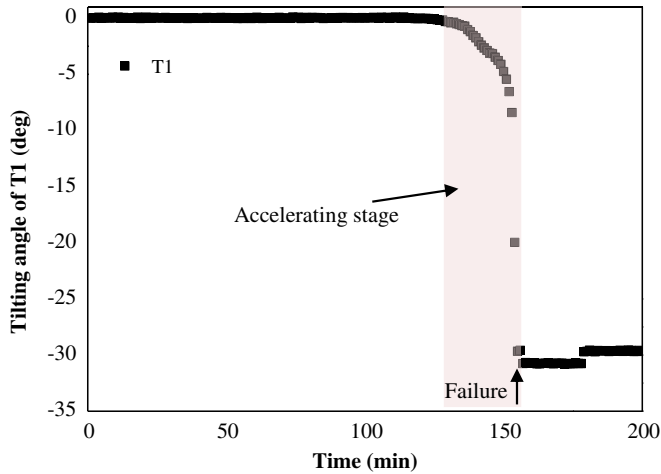


Fig. 15 Time history of tilting of the slope surface measured by T1

T1 was installed. Subsequently, tilt sensor T3 tilted down suddenly since the local failure occurred at the vicinity of T3. There is no clear accelerating stage indicated in the time history of tilting measured by tilt sensors T2 and T4, because of the influence caused by the deposition of the failed part at the lower part of the slope. The initiation of the progressive slope failure in this test was detected by tilt sensor T1, which tilted forward when the slope was sliding. The time history of tilting measured by T1 is presented in Fig. 15, and a clear accelerating stage of tilting is implied before the first slope failure. The relationship between the inverse number of the tilting rate and time in the acceleration stage before slope failure is presented in Fig. 16. A linear trend is revealed in this figure regardless of a deviated point caused by data noises. The predicted slope failure time based on the data of T1 is around 154 min, consistent with the actual failure time of the first slope failure, 155 min.

Results of the field test

The slope failure in the field test was caused by applying artificial rainfall with the rainfall intensity of 21 mm/h. The major failure occurred in the middle part of the natural slope where tilt sensor

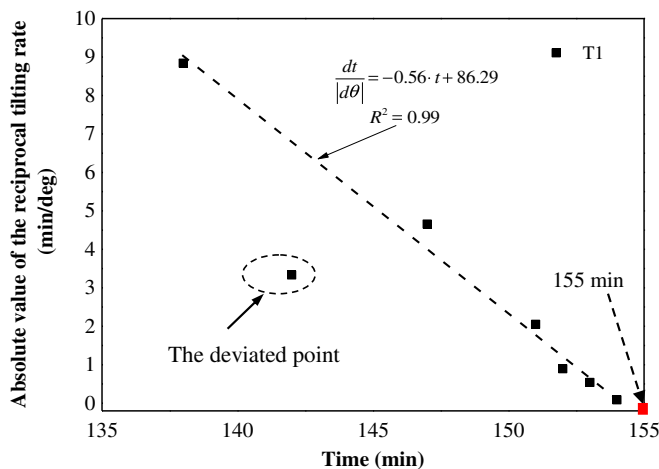


Fig. 16 The reciprocal of tilting rate against time prior to slope failure

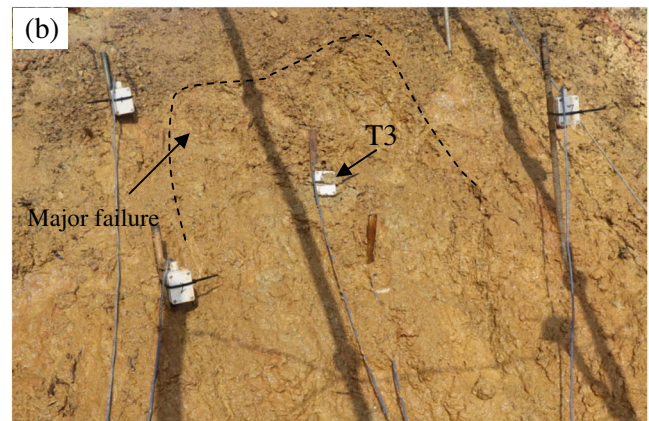


Fig. 17 Images of the field test: (a) The image of the slope before failure, (b) The image of the slope after failure

T3 together with a rod of 7 cm was installed. The failed part slid along the slip surface with a depth of 23 cm as shown in Fig. 6(a). The images of the slope before and after the failure are provided in Fig. 17, while Fig. 18 shows the cumulative tilting angle measured by tilt sensors, and an acceleration stage was detected by T3

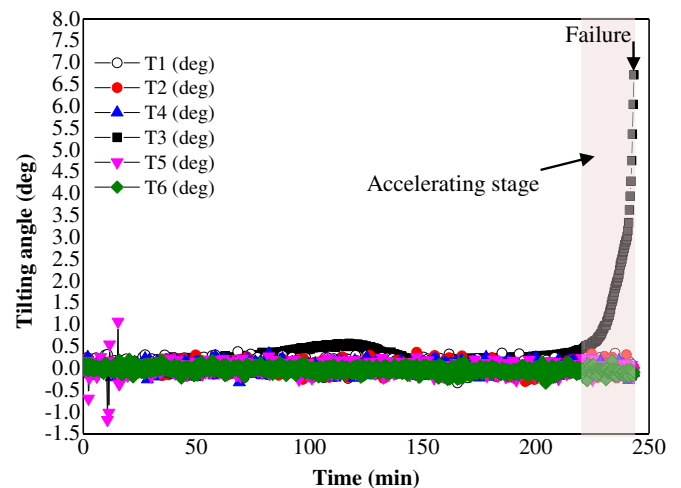


Fig. 18 Time history of tilting of the slope surface

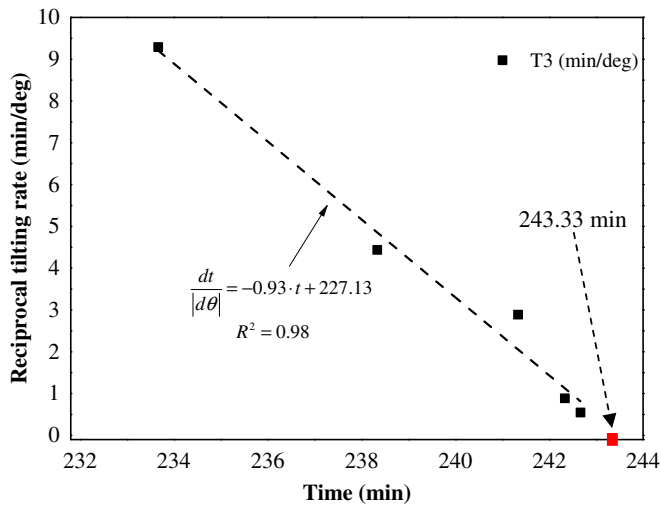


Fig. 19 The reciprocal tilting rate against time prior to slope failure

located in the failed part. T3 tilted backward when the slope was sliding, and the result is implied in Fig. 18. Figure 19 reveals the relationship between the reciprocal tilting rate and time in the acceleration stage of tilting before the slope failure, and a linear trend is also indicated in this figure, consistent with the test results mentioned before. The predicted failure time was calculated based on the fitting line of T3 as shown in Fig. 19, which is 243.54 min coinciding with the actual slope failure time, 243.33 min.

Discussions

The tilt sensors in Model Test 1, T1 and T2, which were set in the surface layer above the slip surface as shown in Fig. 2, tilted backward when the slope was sliding, and positive tilting angles were obtained (Fig. 8). On the other hand, the tilt sensors in Model Test 2, together with a rod reaching the depth of the slip surface (Fig. 3), tilted forward during the slope sliding, and negative tilting angles were observed as indicated in Fig. 11. In addition, similar to the results in Model Test 2, tilt sensor T1 with the length of 200 mm

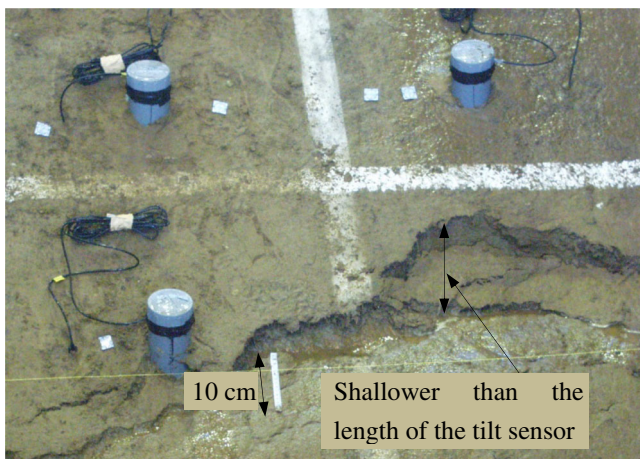


Fig. 20 The initial failure occurred at the toe of the big scale slope model

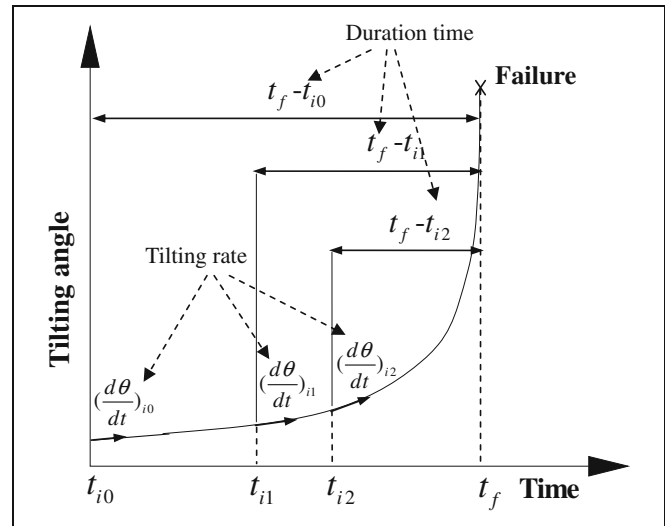


Fig. 21 Definition of the tilting rate and the duration time before slope failure

installed at the lower part of the slope in Model Test 3, also tilted forward, and the depth of the slip surface near T1 was less than 200 mm as shown in Fig. 20. In the field test, the major failure occurred in the middle part of the test slope, and the depth of the slip surface is around 230 mm. The pre-failure tilting behaviors of the sliding mass were detected by tilt sensor T3 which was attached to a rod of 70 mm. The test results as shown in Fig. 18 imply that T3 also tilted backward when the slope was sliding, consistent with the results revealed in Model Test 1.

The results in Model Test 1 and the field test indicate that the tilt sensors, which were located above the slip surface of the landslips with rotational components, moved together with the unstable mass and tilted backward when the slopes were sliding. On the other hand, the results in Model Test 2 and Model Test 3 imply that the tilt sensors together with rods reaching the depth of slip surface tilted forward, and this tilting behavior was caused by the thrust of the moving mass during

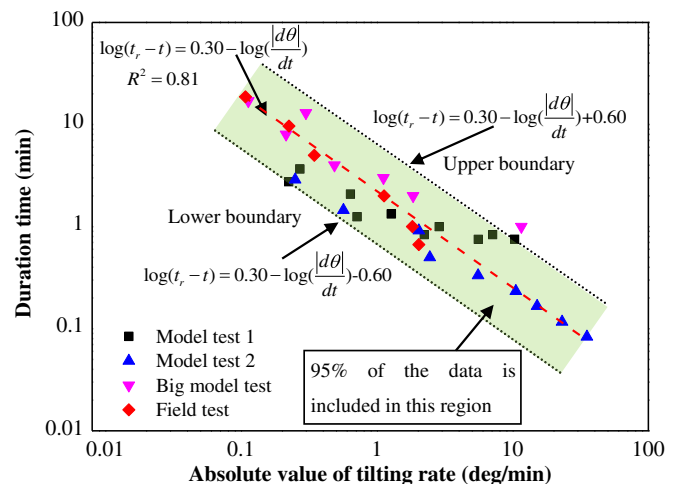


Fig. 22 The relationship between the absolute value of the tilting rate and duration time before slope failure

the slope sliding. Additionally, the results in Model Test 2 and Model Test 3 also reveal that the progressive slope failure in these tests began at the lower part of the failed masses as shown in Fig. 3 and Fig. 4. The pre-failure behaviors of these landslides could be detected by the tilt sensors with rods installed at the lower part of moving masses.

Furthermore, a linear correlation between the reciprocal tilting rate and time in the acceleration stage of tilting was observed in this study. The equation for the linear correlation was also proposed, which can be written as

$$\frac{dt}{|d\theta|} = \frac{-t}{B} + \frac{t_f}{B} \quad (2)$$

Where $\frac{dt}{|d\theta|}$ is the inverse number of tilting rates, and t means time. B is the angular coefficient derived from the linear relation between the reciprocal tilting rate and time. t_f represents the slope failure time, at which the reciprocal tilting rate is assumed to be 0 min^{-1} ($\frac{dt}{|d\theta|} = 0$).

In this study, Eq. (2) was validated by three typical model tests as well as a field test, and the test results are indicated in Fig. 9, Fig. 12, Fig. 16 and Fig. 19 respectively. These test results imply that the predicted failure time for the occurrence of landslides approached by Eq. (2) is consistent with the actual slope failure time in this study. Moreover, Eq. (2) shows a similar form to the landslide prediction methods based on surface displacement measurements as shown in Eq. (1) when α becomes 2 (Saito 1969; Fukuzono 1985; Voight 1988). The correlation between the landslide prediction method using tilting measurements at slope surfaces, and the forecasting method based on the slope surface displacement monitoring, has been rarely studied, and further researches should be carried out in the future.

Additionally, the relationship between the tilting rate and duration remaining in the acceleration stage of tilting before slope failure was also investigated in this study. The physical meaning of the tilting angle rate and the duration time before the slope failure are presented in Fig. 21. As shown in Fig. 21, the tilting angle rate at t_{ij} is $(\frac{d\theta}{dt})_{ij}$, which can be calculated following the method introduced in Appendix of this study, and the corresponding duration time before the slope failure is defined as the time difference between the slope failure time t_f and the time t_{ij} , which is expressed as $t_f - t_{ij}$ as shown in Fig. 21.

According to Eq. (2), the relationship between the tilting rate and duration time before the slope failure can be written as

$$\frac{|d\theta|}{dt} \cdot (t_f - t) = B' \quad (3)$$

Where $\frac{|d\theta|}{dt}$ is the absolute value of the tilting rate, and $t_f - t$ is the duration time. B' is a constant parameter. Theoretically, the value of B' should be equal to the value of B introduced in Eq. (2).

Additionally, in logarithmic space, Eq. (3) can be rewritten as Equation ID=t=t b 15pt

$$\log(t_f - t) = -\log\left(\frac{|d\theta|}{dt}\right) + \log B' \quad (4)$$

The authors plotted the tilting rate against the duration time in logarithmic space as shown in Fig. 22, and the data in this figure

were derived from the tests presented in this study. Figure 22 reveals that the duration time decreases with the increase of the tilting rate, and it also implies a linear trend between the tilting rate and duration time in logarithmic space. The relation for this linear trend based on Eq. (4) is also presented in Fig. 22, and the coefficient of determination (R^2) is 0.81. The expression for the relation is given as Equation ID=t=t

$$\log(t_f - t) = -\log\left(\frac{|d\theta|}{dt}\right) + 0.30 \quad (5)$$

This fitting result gives the validation of Eq. (4). Additionally, Fig. 22 also indicates that most data is situated in a region with clear boundaries. In this study, the region was defined to contain 95% of the data sets, and the formulas for the boundaries of this region can be given as Equation ID=t=t b 10pt

$$\log(t_f - t) = -\log\left(\frac{|d\theta|}{dt}\right) + 0.30 \pm 0.60 \quad (6)$$

Equation (6) can be considered as a potential method to evaluate the duration time within a range at an arbitrary tilting rate in the pre-failure stage. With the increase of data volumes, the precision of the formulas presented in Fig. 22 can be improved, as well as the confidence in evaluation of the duration time at any specific value of $\frac{|d\theta|}{dt}$.

Conclusions

In this paper, the pre-failure tilting behaviors of slopes before slope failure were investigated by performing a series of model tests and a field test. Detailed investigations on the prediction method for the occurrence of landslides based on the tilting monitoring at slope surfaces were also carried out. The major findings of this study are presented as follows,

- 1) The tilt sensor located above the slip surface of the landslides with rotational components, tilted backward when the slope was sliding, while the tilt sensor together with a rod reaching the slip surface of slopes tilted forward in the failure process.
- 2) Based on the results of this study, the initiation of the progressive slope failure can be detected by using tilt sensors with rods installed at the lower part of moving masses.
- 3) A linear relationship between the reciprocal tilting rate and time in the acceleration stage of tilting at the slope surface was observed in this study, and the equation for this linear relationship was also proposed as shown in Eq. (2). The failure time for the occurrence of the slope failure can be forecasted using Eq. (2) by assuming that the inverse number of the tilting rate becomes 0 min^{-1} .
- 4) A linear trend between the tilting rate and duration time before slope failure in logarithmic space was detected, and the expression for this linear trend is given as Eq. (4).
- 5) The authors also provided a potential method to evaluate the duration time within a range at any arbitrary tilting rate in the acceleration stage by using Eq. (6) in this study.>

Acknowledgements

This research was supported by Chinese Scholarship Council (CSC, Grant No.201506370052) for PhD studies of the first author, and the Grants-in-Aid for Scientific Research of the Japan Society for the Promotion of Science (JSPS), Core-to-Core Program B (No. 16H04407).

Appendix

1) The method for the calculation of tilting rates >

In this study, the data series for analyzing were selected with an interval of 1° in the accelerating stage before slope failure considering the influence of noises as well as the fluctuation of the monitoring data which is close to 1° . As shown in Fig. 23, the tilting rate can be approximated using the following equation

$$\left(\frac{d\theta}{dt}\right)_{ij} = \frac{d\theta}{(t_{ij} - t_{ij-1})} \quad (ij = i_1, i_2, \dots, i_n) \quad (A-1)$$

Where t_{ij} and t_{ij-1} represent time, and $d\theta$ means the increment of tilting angles during the period from t_{ij-1} to t_{ij} , in this study, $d\theta = 1^\circ$. $\left(\frac{d\theta}{dt}\right)_{ij}$ is the tilting rate at time t_{ij} .

Then the reciprocal tilting rate can be expressed as

$$\left(\frac{dt}{d\theta}\right)_{ij} = \frac{(t_{ij} - t_{ij-1})}{d\theta} \quad (ij = i_1, i_2, \dots, i_n) \quad (A-2)$$

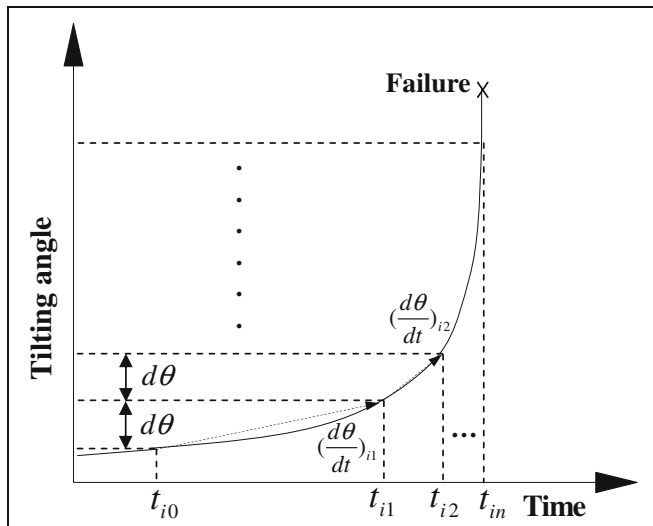


Fig. 23 The method of data selection for analysis in the accelerating stage of slope failure

References

Angeli MG, Pasuto A, Silvano S (2000) A critical review of landslide monitoring experiences. *Eng Geol* 55(3):133–147

- Carlà T, Intrieri E, Di TF, Nolesini T, Gigli G, Casagli N (2017) Guidelines on the use of inverse velocity method as a tool for setting alarm thresholds and forecasting landslides and structure collapses. *Landslides* 14(2):517–534
- Dikshit A, Satyam DN, Towhata I (2018) Early warning system using tilt sensors in Chibho, Kalimpong, Darjeeling Himalayas, India. *Nat Hazards* 94(2):727–741
- Dixon N, Smith A, Flint JA, Khanna R, Clark B, Andjelkovic M (2018) An acoustic emission landslide early warning system for communities in low-income and middle-income countries. *Landslides* 15(8):1631–1644
- Federico A, Popescu M, Murianni A (2015) Temporal prediction of landslide occurrence: a possibility or a challenge? *Italian J Eng Geol Environ* 1:41–60
- Fukuzono T (1985) A new method for predicting the failure time of a slope. *Proc. IV, international conference and field workshop on landslides, Tokyo*, pp 145–150
- García A, Hördt A, Fabian M (2010) Landslide monitoring with high resolution tilt measurements at the Dollendorfer Hardt landslide, Germany. *Geomorphology* 120(1–2):16–25
- Hao SW, Liu C, Lu CS, Elsworth D (2016) A relation to predict the failure of materials and potential application to volcanic eruptions and landslides. *Sci Rep* 6(27877):1–7
- Intrieri E, Gigli G (2016) Landslide forecasting and factors influencing predictability. *Nat Hazards Earth Syst Sci* 16:2501–2510
- Intrieri E, Gigli G, Mugnai F, Fanti R, Casagli N (2012) Design and implementation of a landslide early warning system. *Eng Geol* 147(148):124–136
- Intrieri E, Carlà T, Gigli G (2019) Forecasting the time of failure of landslides at slope-scale: a literature review. *Earth Sci Rev* 193:333–349
- Ishihara Y, Kobatake S (1979). Run off model of flood forecasting. *Bulletin of the Disaster Prevention Research Institute, Kyoto University*, 29: 27–43
- Keefer DK, Wilson RC, Mark RK, Brabb EE, Brown W, Ellen SD, Harp EL, Wiecezorek GF, Alger CS, Zatklin RS (1987) Real-time landslide warning during heavy rainfall. *Science* 238:921–925
- Koerner RM, McCabe WM, Lord AE (1981) Acoustic emission behaviour and monitoring of soils. In *Acoustic emission in geotechnical practice*. ASTM STP 750:93–141
- Kuramoto K, Noro T, Osanai N, Kobayashi M, Okada K (2005). A study on rainfall indexes for giving early warning information for sediment-related disasters. *Proceedings of annual research meeting in 2005, Japan Society of Erosion Control Engineering*, pp 186–187 (in Japanese)
- Manconi A, Giordan D (2016) Landslide failure forecast in near-real-time. *Geomat Nat Haz Risk* 7(2):639–648
- Mufundirwa A, Fujii Y, Kodama J (2010) A new practical method for prediction of geomechanical failure-time. *Int J Rock Mech Min Sci* 47(7):1079–1090
- Okada K (2001). Soil water index Sokko-Jiho. *Japan Meteorological Agency* 69-567-100 (in Japanese)
- Okamoto T, Larsen JO, Matsuura S, Asano S, Takeuchi Y, Grande L (2004) Displacement properties of landslide masses at the initiation of failure in quick clay deposits and the effects of meteorological and hydrological factors. *Eng Geol* 72:233–251
- Osanai N, Shimizu T, Kuramoto K, Kojima S, Noro T (2010) Japanese early-warning for debris flows and slope failure using rainfall indices with radial basis function network. *Landslides* 7(3):325–338
- Petley DN (2012) Global patterns of loss of life from landslides. *Geology* 40:927–930
- Petley DN, Bulmer MH, Murphy W (2002) Patterns of movement in rotational and translational landslides. *Geology* 30(8):719–722
- Petley DN, Mantovani F, Bulmer MH, Zannoni A (2005) The use of surface monitoring data for the interpretation of landslide movement patterns. *Geomorphology* 66:133–147
- Rouse C, Styles P, Wilson SA (1991) Microseismic emissions from flowslide-type movements in South Wales. *Eng Geol* 31(1):91–110
- Saito M (1969). Forecasting time of slope failure by tertiary creep, in: *Proceedings of 7th international conference on soil mechanics and foundations engineering*. Montreal, Canada, Pergamon Press, Oxford, Great Britain, pp 667–683
- Saito M (1987) On application of creep curves to forecast the time of slope failure. *J Jpn Landslide Soc* 24:30–38
- Smethurst JA, Smith A, Uhlemann S, Wooff C, Chambers J, Hughes P, Lenart S, Saroglou H, Springman SM, Löfroth H, Hughes D (2017) Current and future role of instrumentation and monitoring in the performance of transport infrastructure slopes. *Q J Eng Geol Hydrogeol* 50:271–286
- Smith A, Dixon N, Meldrum P, Haslam E, Chambers J (2014) Acoustic emission monitoring of a soil slope: comparisons with continuous deformation measurements. *Géotechnique Lett* 4:255–261
- Towhata I, Uchimura T, Gallage CPK (2005). On early detection and warning against rainfall-induced landslide. *Proc. of the first general assembly and the fourth session of Board of Representatives of the international consortium on landslides (ICL)*, Springer, Washington, DC, pp 133–139

- Uchimura T, Towhata I, Trinh TLA, Fukuda J, Carlos JBB, Wang L, Seko I, Uchida T, Matsuoka A, Ito Y, Onda Y, Iwagami S, Kim MS, Sakai N (2010) Simple monitoring method for precaution of landslides watching tilting and water contents on slopes surface. *Landslides* 7(3):351–357
- Uchimura T, Towhata I, Wang L, Nishie S, Yamaguchi H, Seko I, Qiao J (2015) Precaution and early warning of surface failure of slopes by using tilt sensors. *Soil Foundation* 55(5):1086–1099
- Voight B (1988) A method for prediction of volcanic eruptions. *Nature* 332:125–130
- Voight B (1989) A relation to describe rate-dependent material failure. *Science* 243:200–203
- Xie JR, Uchimura T, Chen P, Liu JP, Xie CR, Shen Q (2019) A relationship between displacement and tilting angle of the slope surface in shallow landslides. *Landslides* 16(6):1243–1251
- Zhang FY, Huang XW (2018) Trend and spatiotemporal distribution of fatal landslides triggered by non-seismic effects in China. *Landslides* 15(8):1663–1674

J. Xie · S. Qiao

Department of Civil Engineering,
Central South University,
Changsha, 410075, Hunan province, China

S. Qiao

e-mail: qiaoshifan@163.com

J. Xie · Z. Maqsood

Department of Civil Engineering,
The University of Tokyo,
7-3-1, Hongo, Bunkyo-ku, Tokyo, 113-8656, Japan

T. Uchimura · S. Tao

Department of Civil and Environmental Engineering,
Saitama University,
255 Shimo-Okubo, Sakura-ku, Saitama, 338-8570, Japan

G. Wang

Disaster Prevention Research Institute,
Kyoto University,
Uji, Kyoto, 611-0011, Japan

Q. Shen (✉) · J. Liu

Department of Civil Engineering,
Hunan University of Technology,
Zhuzhou, 412000, Hunan, China
Email: shenquan123456@csu.edu.cn

Q. Shen · C. Xie · W. Lei · P. Chen · H. Dong · G. Mei

College of Civil Engineering and Architecture,
GuangXi University,
Nanning, 530004, China